

Kinetics of the gas–slurry methanol–higher alcohol synthesis from CO/CO₂/H₂ over a Cs–Cu/ZnO/Al₂O₃ catalyst, including simultaneous formation of methyl esters and hydrocarbons

B.B. Breman, A.A.C.M. Beenackers *, H.A. Schuurman, E. Oesterholt

Department of Chemical Engineering, University of Groningen, Nijenborgh 4, 9747 AG Groningen, Netherlands

Abstract

First kinetic results are presented for the gas–slurry methanol–higher alcohol synthesis from CO/CO₂/H₂ (syngas) over a Cu_{0.44}Zn_{0.43}Al_{0.12}Cs_{0.031} catalyst (particle size: 50–75 μm), slurried in n-octacosane. Experimental conditions varied as follows: pressure = 20–80 bar, temperature = 473–573 K, H₂/CO ratio in the feed = 0.53–3.38, mole fraction CO₂ in the feed = 0.026–0.037 and space velocity = 0.065 × 10^{−3}–1.395 × 10^{−3} Nm³ s^{−1} kg_{cat}^{−1}. Methanol was the major product. Further, higher 1-alcohols, 2-methyl-1-alcohols, methyl esters, n-paraffins, CO₂ and H₂O were formed. In contrast to observations in a gas–solid system, formation of 2-methyl-n-paraffins was negligible. From the same model, proposed earlier for the gas–solid systems B.B. Breman et al., Chem. Eng. Sci., 49, 24A (1995), the product distributions of the alcohols, the paraffins and the methyl esters could be predicted with average relative deviations of 5.9%, 7.8% and 1.6%, respectively. The presence of n-octacosane as a slurry liquid appeared to affect substantially both the product distributions and the values of the model parameters relative to the corresponding gas–solid system.

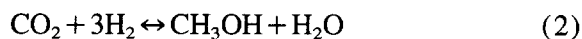
1. Introduction

A methanol–higher alcohol mixture can replace tetraethyl lead as an octane booster in gasoline. Alternatively, it may substitute gasoline to the benefit of the environment and, where natural gas is present, to the benefit of a country [1]. The higher alcohols are required to prevent separation of methanol from gasoline in cold weather [2].

With a suitable catalyst, methanol and higher alcohols can be produced simultaneously from a CO/CO₂/H₂ mixture (syngas) via similar processes as in use for the methanol synthesis (gas-solid or gas–slurry processes [3,4]), also at similar pressures and temperatures ($P = 10$ –100

bar, $T = 473$ –573 K). The following overall reactions play a role:

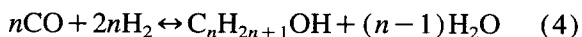
methanol synthesis:



water-gas-shift reaction:



higher alcohol synthesis:



* Corresponding author.

Additionally, other overall reactions for the higher alcohol formation and many side reactions [5] may also be important.

In the conventional gas–solid processes for the methanol synthesis, syngas is passed through a fixed-bed of catalyst particles, implemented either in an adiabatic quenched bed reactor system [6] or a cooled multi-tubular reactor system [7]. In the gas–slurry process the syngas is passed through a slurry of small catalyst particles suspended in an inert, high-boiling liquid. For the methanol synthesis Sherwin and Frank [8] and Sherwin and Blum [9] claimed such a gas–slurry process to have the following advantages relative to conventional gas–solid processes:

- excellent temperature control,
- no diffusion limitations,
- low pressure drop over the reactor,
- low gas recycle ratio,
- efficient energy economy.

In addition, much higher syngas conversions per pass (up to almost 100%) can be achieved for the methanol synthesis by stripping product from a recirculating liquid or slurry stream [10]. The discussed advantages might also be important in the methanol–higher alcohol synthesis.

In general, the presence of the liquid can effect the intrinsic reaction rates of a heterogeneously catalyzed reaction by [11]:

(1) competitive adsorption of the liquid on active catalyst sites,

(2) significant intermolecular interactions between the liquid and the adsorbed reactants, products and intermediate species.

In addition, the presence of a liquid can also affect the catalyst aging (3) [11]. Effect (1) always decreases the reaction rate. Effect (2) can be of importance in case of weakly adsorbed surface species, because then the intermolecular interactions between the liquid and the surface species are relatively high and might affect the reaction rate. Of interest here are the studies of Sattersfield and Stenger [11] on the gas–slurry Fischer–Tropsch synthesis over a reduced fused magnetite catalyst, suspended in various liquids, and the studies of Graaf et al. [3,4] on the low-pressure

gas–solid and gas–slurry methanol synthesis over a commercial Cu/ZnO/Al₂O₃ catalyst. Sattersfield and Stenger [11] observed the reaction rate for CO + H₂ conversion to be about two times higher in phenanthrene than in n-octacosane or in triphenyl methane, whereas in the latter two liquids this reaction rate turned out to be almost equal to that observed in a gas–solid system. Also, Graaf et al. [3,4] observed that the addition of a liquid phase (squalane) significantly affects the various kinetic parameters of the methanol synthesis reaction rate equations. As a result, methanol formation from CO₂ appeared to be the dominant reaction in the gas–slurry system, whereas most methanol is formed from CO in the gas–solid system. Furthermore, the reaction rate of the water-gas-shift reaction (3) appeared to be significantly lower in the gas–slurry system. In case of reactions, the selectivities can also be affected by the presence of a liquid because of intermolecular interactions between the liquid with the surface species (effect (2)) and/or with the various catalyst sites (effect (1)). For example, Sattersfield and Stenger [12] observed higher oxygenate selectivities below 523 K in phenanthrene than in octacosane and triphenyl methane. In contrast, the olefin:paraffin ratios appeared to be hardly affected by the type of liquid. Apparently, the chemical nature of the applied slurry liquid gives an extra parameter to control reaction rates and selectivities in gas–slurry systems relative to gas–solid systems.

In a previous study [13] we reported on the kinetics of the gas–solid methanol–higher alcohol synthesis over a Cs-promoted Cu/Zn/Al₂O₃ catalyst. A new model (PDMCuZn model; Product Distribution Model for synthesis gas conversion over Cu/Zn-based catalysts) proved to be superior to all available literature models [14–16] in predicting the experimental product distributions of both the alcohols and the methyl esters. In addition to the existing models, this model also includes the simultaneous formation of hydrocarbons satisfactorily. The PDMCuZn model is based on the reaction network shown in Fig. 1. See Ref. [13] for the distribution equations of the

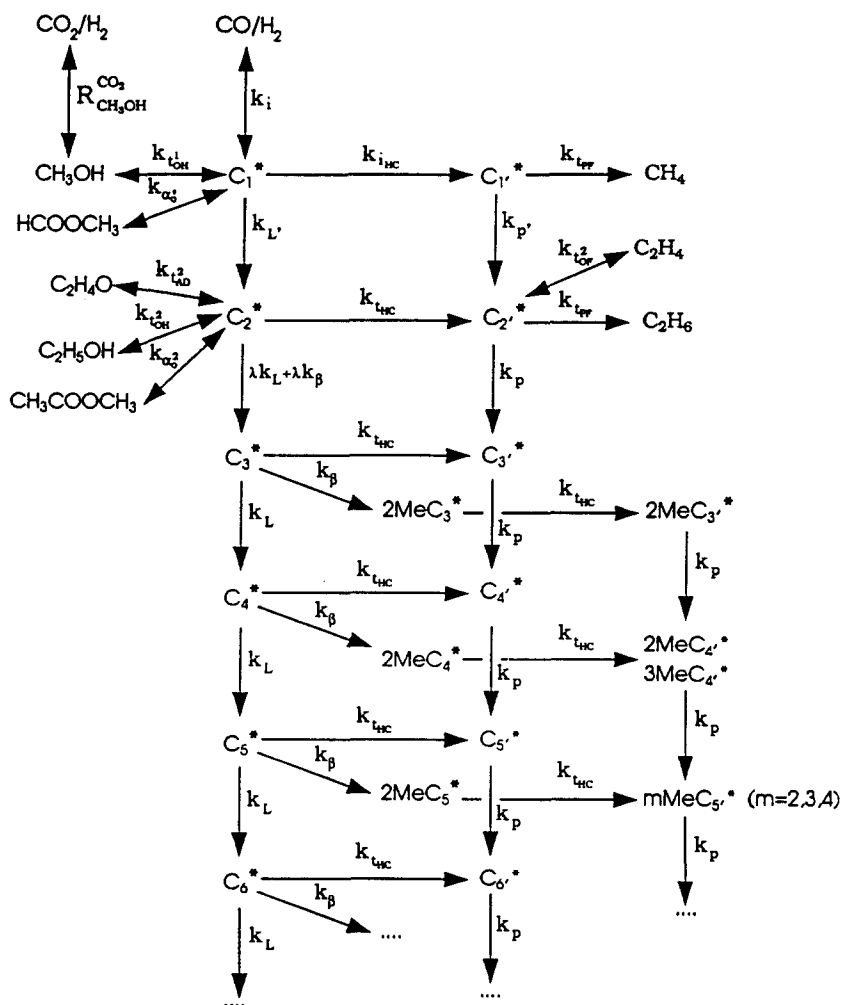


Fig. 1. Reaction network for methanol–higher alcohol synthesis and simultaneous hydrocarbon and oxygenate formation from CO/CO₂/H₂ over Cu/ZnO-based catalysts. For simplicity, termination reactions resulting in gas phase products are given for the various types of C₁ and C₂ precursors only. For all C₃+ precursors, including the branched 2MeC_n precursors, the termination reactions are the same as for the related C₂ precursor.

PDMCuZn model. The parameters in the distribution equations (\bar{L}' , L , β_1 , λ , α_0 , α_0^2 , t_{HC} , \bar{t}_{HC} , p' and p) represent ratios of pseudo first-order kinetic rate constants (for example: $L = k_L/k_{t,OH}$) and are therefore pressure, temperature and composition dependent [13]. As a result, their values have to be determined for each experiment individually. A liquid may affect the rates of the various surface reactions, see above, and thus the parameters of the PDMCuZn model. However, the reaction mechanisms usually remain the same for the gas–slurry system and for the gas–solid system [3,4,12]. Therefore, the PDMCuZn model prob-

ably also holds for the gas–slurry system of this study.

Various authors have reported product distributions for methanol–higher alcohol synthesis over Cu/ZnO-based catalysts in gas–solid reactors [13,15–22]. However, as far as we know, no kinetic data are available to date for methanol–higher alcohol synthesis over a Cu/ZnO-based catalyst in gas–slurry systems, despite its potential, see above. Therefore, the aim of this study is to present initial kinetic data for gas–slurry methanol–higher alcohol synthesis over a Cs–Cu/ZnO/Al₂O₃ catalyst, including the simultaneous

formation of hydrocarbons and methyl esters. A further aim is to test the adequacy of the PDMCuZn model to predict the experimentally observed product distributions. Finally, the influence of the liquid (n-octacosane) on the product distributions and the various model parameters is discussed.

2. Experimental

2.1. Experimental set-up

The present study was carried out in the same well-mixed, gas-slurry reactor used by Graaf et al. [4]. A detailed reactor description is given in Ref. [4]. The reactor was filled with a slurry of 25.6 g of crushed Cs-promoted Cu/ZnO/Al₂O₃ catalyst pellets ($50\ \mu\text{m} < d_p < 75\ \mu\text{m}$) in 128.8 g n-octacosane (purity > 99%), which was kept in batch during the experiments. The catalyst was the same as that used in the previous gas-solid study (composition; Cu_{0.44}Zn_{0.43}Al_{0.12}Cs_{0.031}; see Ref. [13]). Both the slurry and gas section of the reactor were continuously stirred mechanically at a speed of 20 rev s⁻¹. As verified both experimentally and theoretically, a stirring speed of 20 rev s⁻¹ is sufficient to achieve a perfect mixing of gas and slurry, adequate suspension of the solid particles (see also Ref. [5]) and to avoid any heat and mass transfer limitations between the gas and liquid and between the liquid and catalyst particles

for the present system under all conditions applied.

The gas-slurry reactor was placed in the same experimental set-up as applied earlier to study gas-solid kinetics [13]. For a detailed description of the experimental set up, see Ref. [13]. For details on the applied Gas-Solid Chromatographic (GSC) analysis, see also Refs. [13,23].

2.2. Experiments

Before starting the experiments, the catalyst was reduced with a 5 mol-% H₂/95% mol He mixture, passed through the reactor with a flow of $0.1 \times 10^{-3}\ \text{Nm}^3\ \text{s}^{-1}$ at 3 bar. Immediately after starting the reduction procedure, the reactor temperature was increased with a rate of 1/60 K s⁻¹ from 293 K to 513 K. The temperature was kept at 513 K until the water fraction in the reactor outlet flow dropped below the detection limit (after ± 10 hours), indicating a complete reduction. Subsequently, the standard syngas feed 1 (see Table 3) was fed for 4 days at the following conditions: $\Phi_V^{\text{out}} = 0.33 \times 10^{-3}\ \text{Nm}^3\ \text{kg}_{\text{cat}}^{-1}\ \text{s}^{-1}$, $T = 513\ \text{K}$ and $P = 40\ \text{bar}$. After this period, the composition of the product stream became constant and the experimental program could be started.

Table 1 gives an overview of the experimental conditions applied. The purities of the components, from which the syngas feed was pre-fabricated, were: H₂ $\gg 99.999\ \text{mol}\%$, CO $\gg 99.0$

Table 1

Experimental conditions for the kinetic gas-slurry experiments. Slurry: 25.6 g crushed Cs-Cu/ZnO/Al₂O₃ catalyst ($50\ \mu\text{m} < d_p < 75\ \mu\text{m}$) suspended in 128.8 g n-octacosane

Feed number	Composition feed			P (bar)	T (K)	$10^3\ \Phi_V^{\text{out}}/W_{\text{cat}}^{\text{b}}$ (Nm ³ s ⁻¹ kg _{cat} ⁻¹)
	y _{CO}	y _{CO2}	y _{H2}			
1 ^a	0.375	0.0371	0.588	± 40	± 513	± 0.37
1	0.375	0.0371	0.588	20.1–79.5	511–571	0.065–0.38
2	0.405	0.0315	0.563	20.0–59.7	472–570	0.068–1.19
3	0.220	0.0369	0.743	19.9–59.7	471–571	0.070–1.21
4	0.479	0.0261	0.495	39.9–59.8	531	± 0.37
5	0.517	0.0335	0.450	39.9	471–570	0.082–0.38
6	0.636	0.0259	0.338	39.9	471–570	± 0.37

^a Reference conditions for standard experiments.

^b m³ s⁻¹ kg_{cat}⁻¹ at 1 bar, 20°C.

mol-% and $\text{CO}_2 \gg 99.999$ mol-%. A ‘standard’ experiment (see also Table 1) was repeated periodically to determine the catalyst deactivation patterns. After changing the experimental conditions, a certain time interval was required to re-establish steady-state conditions. Assuming both the gas and liquid phase to be ideally mixed and no gas–liquid mass transfer limitations to be present, the time required to approach a new steady-state within 1%, t_i^{exp} , follows from:

$$t_i^{\text{exp}} = 5 \frac{1.013 \times 10^5 (PV_G + m_i PV_L)}{RT \Phi_V^{\text{out}} \times C_G} \quad (5)$$

with V_G and V_L = the volumes of gas and liquid in the reactor, P = reactor pressure (bar), Φ_V^{out} = volumetric flow at 1 bar and $T = 293$ K ($\text{Nm}^3 \text{ s}^{-1}$), C_G = the gas phase concentration (mol m^{-3}) at 1 bar and $T = 293$ K and m_i = gas–liquid solubility (C_{iL}/C_{iG}). t_i^{exp} strongly depends on m_i . To restrict the required experimental time, t_i^{exp} was always taken equal to t_i^{exp} calculated for n-pentanol with, for other reasons [13], a minimum value of 6 hours. After such a period the reactor was stationary for (2-methyl-) 1-alcohols with $n \leq 5$, (2-methyl-) n-paraffins with $n \leq 7$ and all other components with a lower gas–liquid solubility as n-pentanol, including CO , CO_2 , H_2 and H_2O . See Ref. [24] for the relevant m_i values.

3. Results and discussion

43 kinetic experiments, including 6 ‘standard’ experiments, were carried out in a period of 37 days, giving the following set of data: P , T , Φ_V^{out} , y_i ($i = \text{H}_2$, CO , CO_2 , ...). See Ref. [5] for all experimental data. The liquid phase fugacities could be calculated from these data as follows (no mass transfer limitations):

$$f_{iL} = f_{iG} = y_i \varphi_{iG} P \quad (6)$$

with the gas phase fugacity coefficients φ_{iG} in Eq. (6) following from the Soave–Redlich–Kwong equation of state [25].

The most remarkable difference between the present gas–slurry experiments and the previous

gas–solid experiments [13] is the negligible formation of 2-methyl-n-paraffins, indicating a negligible dehydration of alcohols (reaction path k_{THC} in Fig. 1).

The nine relevant parameters of the PDMCuZn model, i.e. \bar{L} , L , β_1 , λ , α_0' , α_0'' , \bar{i}_{HC} , p' and p , were determined from the experimental data by minimizing the χ^2 function with the Levenberg–Marquardt method [26]:

$$\chi^2 = \sum_i \frac{(\bar{y}_i^{\text{exp}} - \bar{y}_i^{\text{mod}})^2}{\sigma_i^2} \quad (7)$$

Here, \bar{y}_i is the ratio of the mole fractions of product i and methanol in the reactor outlet flow:

$$\bar{y}_i = \frac{y_i}{y_{\text{CH}_3\text{OH}}} \quad (8)$$

σ_i was always taken equal to $0.05 \bar{y}_i^{\text{exp}}$, see Ref. [13] for further details. Because an exact fit can always be realized for nine data point only experiments with at least ten data points were considered. The parameters t_{HC} , t_{AD}' and t_{OF}'' were all set at zero because of the negligible formation rates of the corresponding products. Similar to Ref. [13], the number of optimizing parameters could be reduced whenever higher methyl esters, methylformate, C_3+ hydrocarbons and C_2+ hydrocarbons were not significantly present (α_0' , α_0'' , p and p' , respectively, equal to zero). t_{OH}' and α_0' were calculated as described previously for the gas–solid experiments [13].

The accuracy and the adequacy of the optimized PDMCuZn model to predict the experimental product distributions are expressed by the MARR function and the relative standard deviation, respectively:

$$\text{MARR} = \sum_i^N \left| \frac{\bar{y}_i^{\text{exp}} - \bar{y}_i^{\text{mod}}}{\bar{y}_i^{\text{exp}}} \right| \frac{1}{N} \times 100\% \quad (9)$$

$$s_{\text{rel}} = \left[\sum_i^N \left(\frac{\bar{y}_i^{\text{exp}} - \bar{y}_i^{\text{mod}}}{\bar{y}_i^{\text{exp}}} \right)^2 \frac{1}{N-m} \right]^{1/2} \quad (10)$$

with the sums in Eqs. (9) and (10) including all model predictions: $N = \sum_j^{N_{\text{exp}}} N_j$ and $m = \sum_j^{N_{\text{exp}}} m_j$. See Table 2 for the corresponding s_{rel} and MARR

Table 2

Accuracies of the PDMCuZn model for the present gas–slurry study. For comparison, the corresponding accuracies for the gas–solid system are also included [13]

Study	MARR (%) ^a			s^a	N	m
	Alcohols	Methyl esters	Hydrocarbons			
Gas–slurry	5.9	1.6	7.8	16	505	309
Gas–solid	6.7	4.1	9.8	22	764	479

^a The model predictions for all experiments considered are included in Eqs. (9) and (10).

values. For comparison, the corresponding values for the gas–solid experiments [13] are also given in Table 2. Notice from the lower s_{rel} value of the gas–slurry system that the PDMCuZn model is

slightly more accurate for the present gas–slurry study. This is caused by improved model predictions for the methyl esters and the hydrocarbons. Figs. 2a–d show the relative residuals, RR:

$$RR = \left(\frac{\bar{y}_i^{exp} - \bar{y}_i^{mod}}{\bar{y}_i^{exp}} \right) \times 100\% \quad (11)$$

of all model predictions from the PDMCuZn model as a function of \bar{y}_i^{exp} for various types of products. The RR values for methyl formate are not shown in Fig. 2d because these are always zero (one optimizing parameter, α'_0 , for one data point). Fig. 2a–2d shows the PDMCuZn model to predict \bar{y}_i^{exp} mostly within 15% and always within 50% without serious trends in the relative residuals as a function of \bar{y}_i^{exp} . The MARR values and the optimal parameter values for all individual experiments are given elsewhere [5]. The maximal MARR value was only 14.3%.

The Fig. 3a–d show both experimental and predicted product distributions. For comparison, the corresponding gas–solid data [13] are also shown at similar experimental conditions. Again, the accuracy of the model predictions proves to be very good. Fig. 3a–d also shows that the slurry liquid (n-octacosane) substantially affects the product distributions. The 1-alcohol : 2-methyl-1-alcohol ratios ($n \geq 4$), the $C_{n+1} : C_n$ ratios for 1-alcohols ($n \geq 2$), 2-methyl-1-alcohols ($n \geq 4$) and n-paraffins ($n \geq 2$) and the methane : methanol ratio are all increased by the presence of the liquid. Further, the absence of significant 2-methyl-n-paraffin formation and the relatively high methane : ethane ratios are specific for the slurry system. Fig. 4a–b compares the various gas–slurry model parameter values to the corre-

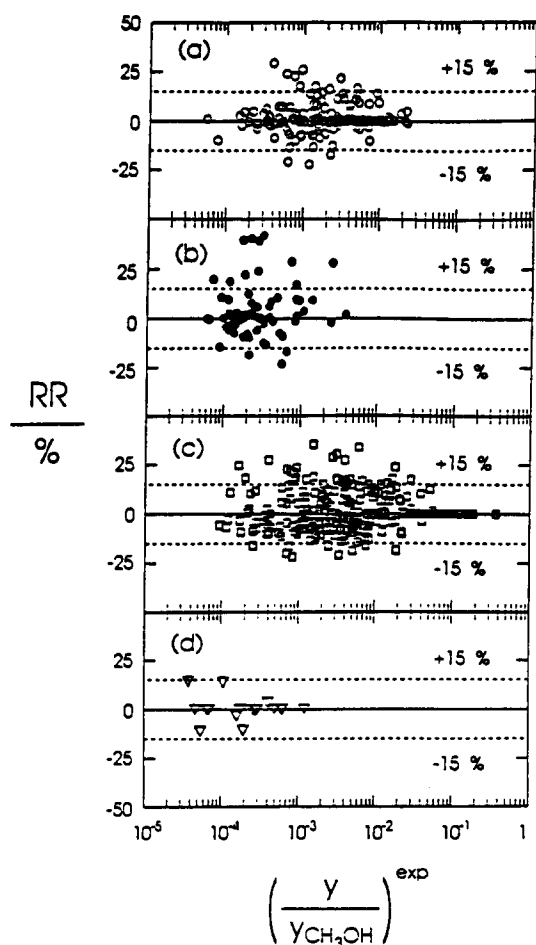


Fig. 2. Relative residuals, RR, of all PDMCuZn model predictions as a function of the experimental relative mole fraction, \bar{y}_i^{exp} . (a) \circ , 1-alcohols; (b) \bullet , 2-methyl-1-alcohols; (c) \square , n-paraffins; (d) ∇ methyl esters.

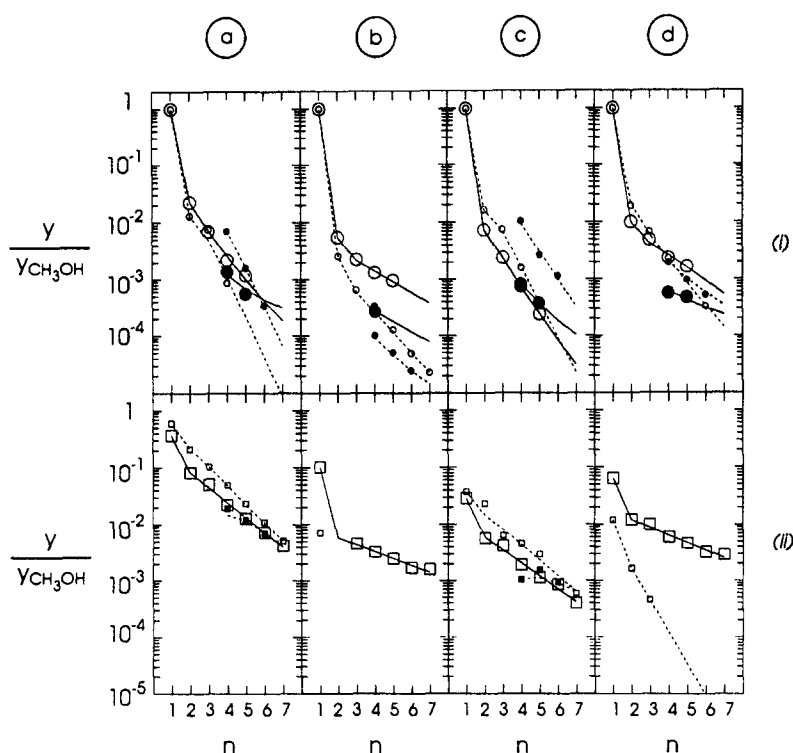


Fig. 3. (a)–(d) Product distributions obtained in a gas–slurry system (this study: large symbols, solid lines) and in a gas–solid system ([13]): small symbols, dashed lines). Symbols are experimental data. Lines are predicted from optimized PDMCuZn model. (i) Product distributions of 1-alcohols (\circ) and 2-methyl-1-alcohols (\bullet). (ii) Product distributions of n-paraffins (\square) and 2-methyl-n-paraffins (\blacksquare). Experimental conditions ($H_2/CO = y_{H_2}/y_{CO}$ at the reactor outlet) are shown in Table 3.

sponding gas–solid results [13]. Apparently, the parameters \bar{L}' , β_1 , i_{HC} , t_{HC} and p are most strongly affected by the presence of the liquid, whereas p' , L and λ are less and α'_0 and α_0^2 are hardly affected. Usually, the \bar{L}' values are lower in the gas–slurry system. This, does not necessarily imply lower ethanol : methanol ratios in the gas–slurry system because, due to lower β values, $C_2 \rightarrow C_3$ chain

growth is also relatively slow in the gas–slurry system. The relatively high 1-alcohol : 2-methyl-1-alcohol ($n \geq 4$) and $C_{n+1} : C_n$ ($n \geq 2$) ratios obtained with the gas–slurry system also originate from the lower β values. The different influence of the liquid on \bar{L}' and on L supports the presumption of Breman et al. [13] that different parameters are needed for $C_1 \rightarrow C_2$ and $C_n \rightarrow C_{n+1}$ ($n \geq 2$)

Table 3

Experimental conditions ($H_2/CO = y_{H_2}/y_{CO}$ at the reactor outlet) used in the experimental results shown in Fig. 3.

Figure	System	H_2/CO	P (bar)	T (K)	$10^3 \Phi_{V}^{out}/W_{cat}$ ($Nm^3 s^{-1} kg_{cat}^{-1}$)
3a	Gas–solid	5.3	40	571	0.36
	Gas–slurry	5.8	40	570	0.34
3b	Gas–solid	0.5	40	491	0.37
	Gas–slurry	0.5	40	494	0.33
3c	Gas–solid	1.5	60	551	0.30
	Gas–slurry	2.0	60	550	0.43
3d	Gas–solid	0.5	40	530	0.36
	Gas–slurry	0.5	40	528	0.34

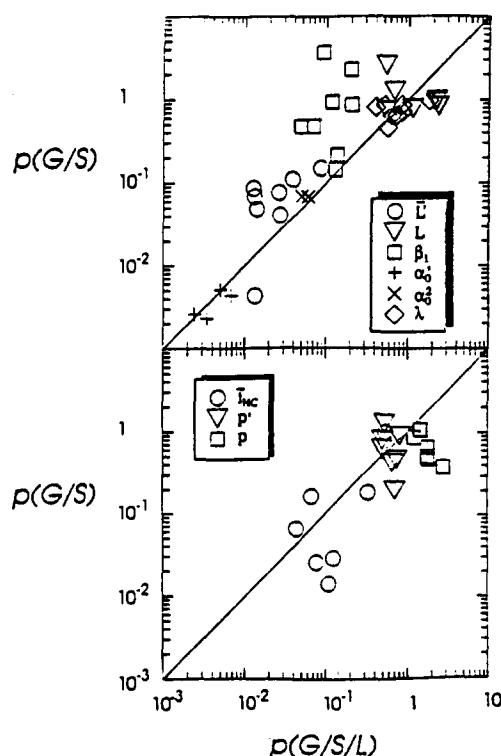


Fig. 4. (a)–(d) PDMCuZn parameter values of the gas–solid system, $p(\text{G/S})$ [13], compared to the corresponding values obtained for the gas–slurry system, $p(\text{G/S/L})$.

chain growth of the oxygenate precursors. This is caused by both different mechanisms for $\text{C}_1 \rightarrow \text{C}_2$ (L') and $\text{C}_n \rightarrow \text{C}_{n+1}$ (L) chain growth and by a significant contribution of the CO_2/H_2 route to methanol formation, $\text{R}_{\text{CH}_3\text{OH}(\text{CO}_2)}$, incorporated in \bar{L}' [13]:

$$\bar{L}' = L' \left(1 + \frac{\text{R}_{\text{CH}_3\text{OH}(\text{CO}_2)}}{k_{\text{rOH}}^1 C_{\text{C}_1}^*} \right)^{-1} \quad (12)$$

The second term between the brackets represents the contribution of the CO_2 to methanol formation relative to that of the CO/H_2 route. Graaf et al. [4] also observed the contribution of the CO_2/H_2 route to be substantially increased by introducing a similar liquid (squalane). This might explain the relatively low \bar{L}' values observed in the gas–slurry system, see Eq. (12), though a retarding effect of the liquid on the $\text{C}_1 \rightarrow \text{C}_2$ (L') chain growth rate relative to that of $\text{C}_n \rightarrow \text{C}_{n+1}$ (L) can not be excluded either. The relatively high meth-

ane : methanol ratios for the gas–slurry system originate from relatively high \bar{t}_{HC} values whereas the relatively higher values of p result in relatively low slopes in the n -paraffin distribution plots for $n \geq 2$ (higher $\text{C}_{n+1} : \text{C}_n$ ratios). In contrast, the lower ethane : methane ratios obtained in the gas–slurry system follow from the relatively high values of p and the zero values of t_{HC} . Possibly, the zero (or negligible) values of t_{HC} originate from blockage of the active catalyst sites for this reaction path by strong liquid adsorption. The different influence of the liquid on p' relative to p supports the presumption of Breman et al. [13] that $\text{C}_n \rightarrow \text{C}_{n+1}$ ($n \geq 2$) chain growth of the hydrocarbon precursors proceeds mainly via a different reaction mechanism than $\text{C}_1 \rightarrow \text{C}_2$ chain growth.

Competitive adsorption of the liquid on active catalyst sites will reduce the reaction rates whereas significant intermolecular interactions between liquid and adsorbed species can either increase or decrease reaction rates, depending on the temperature and the type of liquid. The model parameters in the PDMCuZn model represent ratios of surface reaction rates. Therefore, it is complicated to determine which of the above effects dominates the observed changes in the model parameters. However, Sattersfield and Stenger [11,12] observed n -octacosane to have only a negligible influence on the reaction rates in the Fischer–Tropsch synthesis over a reduced fused magnetite (Fe-based) catalyst, indicating both effects to be negligible. In contrast, Graaf et al. [3,4] observed a significant influence of a similar liquid (squalane) on the various reaction rates in the methanol synthesis over a $\text{Cu}/\text{ZnO}/\text{Al}_2\text{O}_3$ catalyst. The observed methanol production rates were relatively high in the gas–slurry system for $T < \pm 523$ K and relatively low for $T > \pm 523$ K. This behaviour suggests that liquid–adsorbed species interactions are dominant over liquid adsorption on active sites, because the latter is expected to be most pronounced at low temperatures, see above. These differences in the influence of a saturated paraffin as a slurry liquid in the Fischer–Tropsch and in the methanol synthesis might originate from relatively strongly adsorbed surface species

on typical Fischer–Tropsch catalyst [27]. Intermolecular interactions between liquid and adsorbed surface species are thought to be more significant for weakly adsorbed surface species [11].

From the above discussion, we expect (1) competitive adsorption of n-octacosane on active catalyst sites to be negligible with our Cu/ZnO/Al₂O₃-based and (2) n-octacosane to affect substantially the selectivities and the related model parameters via different liquid–adsorbed species interactions. The latter suggests the chemical nature of the slurry liquid to be an additional parameter to control the selectivities in the gas–slurry methanol–higher alcohol synthesis over Cu/ZnO-based catalysts.

4. Conclusions

Initial data are reported on the kinetics of the gas–slurry methanol–higher alcohol synthesis over Cu/ZnO-based catalysts.

The PDMCuZn model, which proved to be the best model for a gas–solid system, can also describe the observed gas–slurry product distributions with average relative deviations of 5.9%, 7.8% and 1.6% for the alcohols, n-paraffins and methyl esters, respectively.

The presence of n-octacosane as a slurry liquid appears to affect the product distributions substantially. Relative to the gas–solid system, the gas–slurry system shows relatively high 1-alcohol : 2-methyl-1-alcohol ratios ($n \geq 4$), relatively high $C_{n+1} : C_n$ ratios for both the 1-alcohols ($n \geq 2$), the 2-methyl-1-alcohols ($n \geq 4$) and the n-paraffins ($n \geq 2$), relatively high methane : ethane ratios, relatively high methane : methanol ratios and negligible 2-methyl-n-paraffin formation.

These differences are reflected by significantly different values of the related PDMCuZn model parameters for the gas–slurry system and the gas–solid system and originate most likely from significant intermolecular interactions between the liquid and the adsorbed surface species.

The different influence of the liquid on the PDMCuZn model parameters \bar{L}' relative to L and p' relative to p is in line with the appearance of different reaction mechanisms for $C_1 \rightarrow C_2$ chain growth and $C_n \rightarrow C_{n+1}$ ($n \geq 2$) chain growth for both the oxygenate and hydrocarbon precursors, as suggested previously [13].

Acknowledgement

The authors acknowledge the financial support of DSM B.V., Geleen, the Netherlands, and the technical support of P. Dijkema, O. Staal and J.H. Marsman.

References

- [1] N.D. Brinkman, E.E. Ecklund and R.J. Nichols, (Editors), Fuel Methanol: A Decade of Progress, Society of Automotive Engineers, Inc., Warrendale, USA (1975).
- [2] H.K. Lee, D.O. Shah and N.D. Brinkman in N.D. Brinkman et al., Enhanced Stability of Methanol–Gasoline Blends.
- [3] G.H. Graaf, E.J. Stamhuis and A.A.C.M. Beenackers, Chem. Eng. Sci., 43 (12) (1988) 3185.
- [4] G.H. Graaf, J.G.M. Winkelman, E.J. Stamhuis and A.A.C.M. Beenackers, Chem. Eng. Sci., 43 (8) (1988) 2161.
- [5] B.B. Breman, The Methanol–Higher Alcohol Synthesis from CO/CO₂/H₂ over Cu-based Catalysts, PhD Thesis, University of Groningen, Groningen, The Netherlands (1995).
- [6] I. Dybkjaer, Chem. Eng. Rev., 13 (6) (1981) 17.
- [7] E. Supp, Hydrocarbon Processing, 3 (1981) 71.
- [8] M.B. Sherwin and M.E. Frank, Hydrocarbon Process., 11 (1976) 122.
- [9] M.B. Sherwin and D. Blum, Liquid-Phase Methanol, EP-RI-AF-693 Research project 317-2 (1978).
- [10] J.M. Berty, C. Krisman and J.R. Elliot, CHEMTECH, (1990) 624.
- [11] C.N. Sattersfield and H.G. Stenger Jr., Ind. Eng. Chem. Process. Des. Dev., 24 (1985) 407.
- [12] C.N. Sattersfield and H.G. Stenger Jr., Ind. Eng. Chem. Process. Des. Dev., 24 (1985) 411.
- [13] B.B. Breman, A.A.C.M. Beenackers and E. Oesterholt, A. Kinetic Model for the Methanol–Higher Alcohol Synthesis from CO/CO₂/H₂ over Cu/ZnO-based Catalysts, including Simultaneous Formation of Methyl Esters and Hydrocarbons, Chem. Eng. Sci., 49, 24A (1995).
- [14] K.J. Smith and R.B. Anderson, J. Catal., 85 (1984) 428.
- [15] G.A. Vedage, P.B. Himmelfarb, G.W. Simmons and K. Klier, Solid-state Chemistry in Catalysis, ACS Symp. Ser., 279 (1985) 295.
- [16] K.J. Smith, C.W. Young, R.G. Herman and K. Klier, Ind. Eng. Chem. Res., 30 (1991) 61.

- [17] K.J. Smith and R.B. Anderson, *Can. J. Chem. Eng.*, 61 (1983) 40.
- [18] H. Fink, Studies on Alcohol Synthesis with a Cu–ZnO Catalyst in a Recycle Reactor, PhD Thesis, Kernforschungsanlage, Jülich, Germany (1988).
- [19] J.G. Nunan, C.E. Bogdan, K. Klier, K.J. Smith, C.W. Young and R.G. Herman, *J. Catal.*, 113 (1988) 410.
- [20] J.G. Nunan, C.E. Bogdan, K. Klier, K.J. Smith, C.W. Young and R.G. Herman, *J. Catal.*, 116 (1989) 195.
- [21] A. Kiennemann, H. Idriss, R. Kieffer, P. Chaumette and D. Durand, *Ind. Eng. Chem. Res.*, 30 (6) (1991) 1130.
- [22] J. Slaa, PhD Thesis, Twente University of Technology, Enschede, The Netherlands (1991).
- [23] J.H. Marsman, B.B. Breman and A.A.C.M. Beenackers, *J. High Resolution Chrom.*, 16 (1993) 141.
- [24] B.B. Breman, A.A.C.M. Beenackers, E.W.J. Rietjens and R.J.H. Stege, *J. Chem. Eng. Data*, 39 (4) (1994) 647.
- [25] G. Soave, *Chem. Eng. Sci.*, 27 (1972) 1197.
- [26] W.H. Press, B.P. Flannery, S.A. Teukolsky and W.T. Vetterling, *Numerical Recipes in Pascal, The Art of Scientific Computing*, Cambridge University Press, USA (1989).
- [27] J.A. Moulijn, P.W.N.M. Van Leeuwen and R.A. Van Santen (Editors), *Catalysis: An Integrated Approach to Homogeneous, Heterogeneous and Industrial Catalysis*, Elsevier, Amsterdam, (1991).